Lafia Journal of Scientific & Industrial Research (LJSIR), Vol. 4(2), 2026
p-ISSN: 3026 - 9288 e-ISSN: 3027 - 1800 pages: 131-138
https://lafiascijournals.org.ng/index.php/ljsir/index ⇒ Published by the
Faculty of Physical Sciences, Federal University of Lafia, Nasarawa State, Nigeria

Bismuth Doped Soda Lime Silica Borate (SLS–B_2O_3–Bi_2O_3) Glasses for Gamma Radiation Shielding Application

Umar Sa'ad Aliyu[1,2]*, Ibrahim Gana Geidam[3], Abdulkarim Muhammad Hamza[1], Sani Muhammad, Mustapha Adejo Muhammad[1], Hassan Shaibatu Ibrahim[4] & Mustapha Bukar Liberty[5]

[1]Department of Physics, Federal University of Lafia, Nasarawa State, Nigeria
[2]Muhammadu Buhari TETFund Center of Excellence, Federal University of Lafia, Nasarawa State, Nigeria
[3]Department of Physics, Yobe State University Damaturu, Nigeria
[4]National Agency for Science and Engineering Infrastructure, Idu, Abuja, Nigeria
[5]Department of Physics, Kashim Ibrahim University, Maiduguri, Borno State, Nigeria

Abstract

In this research, local content of glass waste, pure powdered boron oxide and bismuth oxide as starting materials were utilized for fabrication of glasses. These glasses will serve as safer substitutes to lead blocks/lead glasses and concretes in radiation shielding in industries, research institutes and medical diagnostic centers. The main objective of this work is to study the physical, structural and radiation shielding properties of the glasses. For the glass fabrication, a conventional melt-quenching technique and chemical compositional formula xBi_2O_3-(100-x) [50SLS-$50B_2O_3$], where x = 0, 1, 2, 3, 4, 5 wt% were utilized. Various measurements and characterizations such as density measurement and X-ray diffraction (XRD) were carried out to study the structural and physical properties of the glasses. The gamma shielding measurements were carried out using NaI (TI) detector gamma spectrometer using a Cs-137 point source with photon energy 0.662 MeV. The density value increased from 2.264847 to 2.401604 gcm^{-3}. The XRD spectral pattern showed the amorphous nature of the glasses. The LAC and MAC values ranged between 0.0624 to 0.1277 cm^{-1} and 0.0276 to 0.0532 cm^2/g. Other gamma radiation shielding efficiency parameters studied include Half Value Layers (HVL), Mean Free Path (MFP), Tenth Value Layer (TVL), Permeability Factor (PF) and Radiation Protection Efficiency (RPE).

Keywords: Borate glasses, Soda lime silicate (SLS) glasses, Radiation shielding glasses

Article History

Submitted
July 28, 2026

Revised
September 14, 2026

First Published Online
September 16, 2026

***Correspondences**
U. S. Aliyu
usaltilde@yahoo.com

doi.org/10.62050/ljsir2026.v4n2.911

Introduction

Different types of ionizing radiation such as charged particles, neutron, and γ/X-rays release from the natural background radiation sources such as cosmic rays, internal radiation, and terrestrial radiation or from man-made radiation sources such as chemical reactions, nuclear weapons, and nuclear reactors[1–5]. On the other hand, many vital applications ranging from medical practices to industrial research were affected by development of artificial radiation sources [6].

Radiation shielding glasses have been one of the major areas of focus of glass experts in recent years, owing to their transparent nature and ability to attenuate gamma and x-ray electromagnetic waves[7–10]. There are different materials considered for radiation shielding applications. The most prominent one is the lead which is a heavy metal that is considered toxic, then tiles and concrete materials, which on the other hand degrade and are not transparent [11].

Different researchers have synthesized variety of compositions of glasses in an attempt to achieve efficient and effective gamma and x-ray shielding. Among them include the work of Elsaman *et al*. [12], where PbO–MoO_3–V_2O_5 glasses were synthesized and radiation shielding properties were studied. Abdelgawad *et al*. [13] utilized Cement Bypassed Dust (CBD) to synthesize glass with of composition B_2O_3–Bi_2O_3– V_2O_5–Na_2O - (CBD) for radiation shielding application. Bhavya *et al*. [14] synthesized a system of B_2O_3–TeO_2–Bi_2O_3–BaO–Gd_2O_3/CeO_2 glasses and studied the radiation properties. Azuraida *et al*. [10] synthesized and studied the radiation shielding characteristics of barium boro-tellurite (BaO–B_2O_3–TeO_2) glass system. Alomairy *et al.* [15] presented a study on the synthesis and the study the radiation shielding properties of Nd_2O_3 doped PbF_2–TeO_2–WO_3. Mahmoud *et al*. [5] used both the experimental and theoretical approach in studying the radiation shielding and mechanical properties of SiO_2–Li_2O–CdO–Gd_2O_3–Er_2O_3 glasses synthesized using melt-quenching technique. In another study, Al-Buriahi *et al*. [16] synthesized a system of TeO_2–CaF_2–B_2O_3–CaO glasses and investigated the radiation shielding characteristics of the glasses theoretically using Phy-X and Geant4 simulations tools. These studies investigated the radiation shielding properties of their respective glass composition via determination and analysis of parameters such as linear attenuation coefficient (LAC), Tenth Value Layer (TVL), Mass Attenuation Coefficient

(MAC), Half Value Layer (HVL), Mean Free path (MFP) and others.

In this work, local content of SLS glass waste, pure powdered boron oxide and bismuth oxide as glass starting material were utilized as safer substitutes to lead blocks/glasses and concretes in radiation shielding in industries, research institutes and medical diagnostic centers. The main objective of this work is to investigate the shielding efficiency of the synthesized glasses. Various measurements and characterizations such as density measurement and the X-ray diffraction (XRD). In addition, the study also includes gamma radiation shielding properties of the glasses through the measurement of Linear Attenuation Coefficient (LAC), Mass Attenuation Coefficients (MAC), Half Value Layers (HVL), Mean Free path (MFP), Permeability Factor (PF) and Radiation Protection Efficiency (RPE).

Materials and Methods

Experiments

A series of bismuth soda lime silica borate glass compositions were selected according to the following empirical formula, xBi_2O_3-(100-x)[50SLS-50B_2O_3], where x = 0, 1, 2, 3, 4, 5 wt%. The starting materials were chemical reagents grade Bi_2O_3, B_2O_3 and SLS. 30 g of the chemicals were weighed using an electronic digital balance (±0.0001 g) and mixed for 30 min in a crucible to achieve homogeneity. A pre-heating process was carried out in the first furnace for 1 h at 400 °C to remove excess moisture content. Then transferred to a second electric furnace and melted (at 1100 °C for 3 h). The melt was quenched in a pre-heated cylindrical shape stainless steel split mold and annealed in the first furnace preset at 400 °C for 1 h to minimize thermal shock. The synthesized glass samples were properly polished with different grades of silicon carbide paper (1500, 1200, 800 and 400 mesh) to achieve require thickness, transparency, parallel, and flat surface. Thickness of the glass samples were measured using Vernier caliper. Finally, some proportions of the glass samples were crushed to a fine powdered using pestle and mortar for XRD analysis.

Experimental gamma radiation attenuation measurement was carried out using a lead equivalent thickness (LET) set up. A cesium-137 (137Cs) point source with gamma energy 662 keV and activity 0.9965 mCi was used for testing the radiation shielding effectiveness of the prepared glasses. The radiation attenuation experiment was conducted with a 32 cm source to detector (SSD) distance using lead collimators with 1.5 mm and 0.5 mm apertures to reduce scattered radiation [17]. Background radiation and the initial intensity (I_0) were measured before placing each sample between the collimators. The attenuated intensity (I) was then measured for 60 seconds, with each measurement repeated ten times using a Ludlum survey meter (Model 2241) ± 0.01 mm accuracy [17]. After background correction, the mean values of I_0 and I were used to plot $\ln\left(\frac{I_0}{I}\right)$ against sample thickness. The linear attenuation coefficient (μ) was obtained from the slope of the plot and subsequently used to determine other shielding parameters.

Results and Discussion

Density

Figure 1 and Table 1 respectively present the variations of density and the values for Bi_2O_3 doped SLS borate glasses. The density value increased from 2.264847 to 2.401604 gcm^{-3} as the bismuth oxide composition increased from 0 to 5 %.

The glasses density was determined using equation (1) as presented by Umar *et al.* [18]

$$\rho_{sample} = \frac{w_{air}}{W_{water}} \rho_{water} \qquad (1)$$

Density increase in glasses are usually associated with either substitution of lighter atomic elements with heavier ones, decrease in interstitial spaces between atoms and/or increase in bond networking between the atoms [18–23]. In the case of our glasses, the density might be a result of increase in the overall molar mass of the glasses without a corresponding increase in volume as Bi_2O_3 composition increases in the glass network. Another reason is that the Bi_2O_3 increase in the composition might have increase the glass network connectivity by acting as a glass former instead of a modifier. Bismuth oxide acts as network former in some compositions and as modifier in some other compositions [24, 25].

Table 1: Batch formulation, sample thickness, (cm) and density (gcm^{-3}) of Bismuth oxide doped SLS borate glasses

Sample	50 SLS (g)	50 B_2O_3 (g)	Bi_2O_3 (g)	Total (g)	Thickness (cm)	Density (gcm^{-3})
0	15	15	0	30	0.633	2.264847
1	14.85	14.85	0.3	30	0.512	2.330667
2	14.70	14.70	0.6	30	0.557	2.34224
3	14.55	14.55	0.9	30	0.628	2.350857
4	14. 40	14.40	1.2	30	0.596	2.401604
5	14.25	14.25	1.5	30	0.641	2.409941

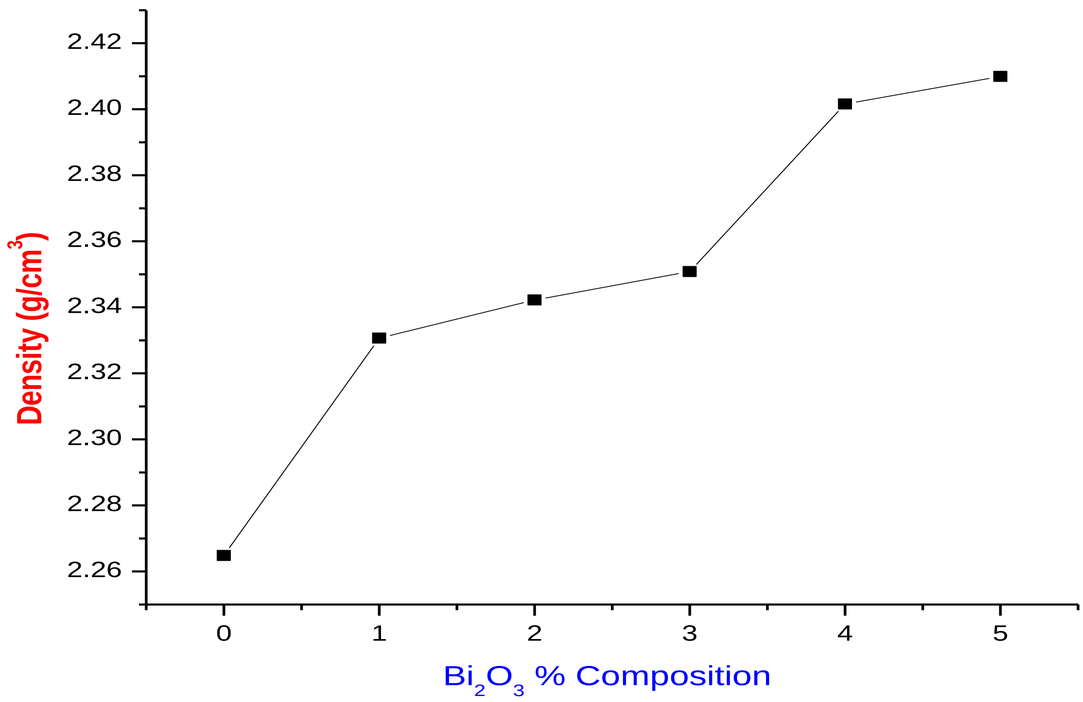

Figure 1: Density variation against Bi_2O_3 % composition of Bi_2O_3 doped SLS borate glasses

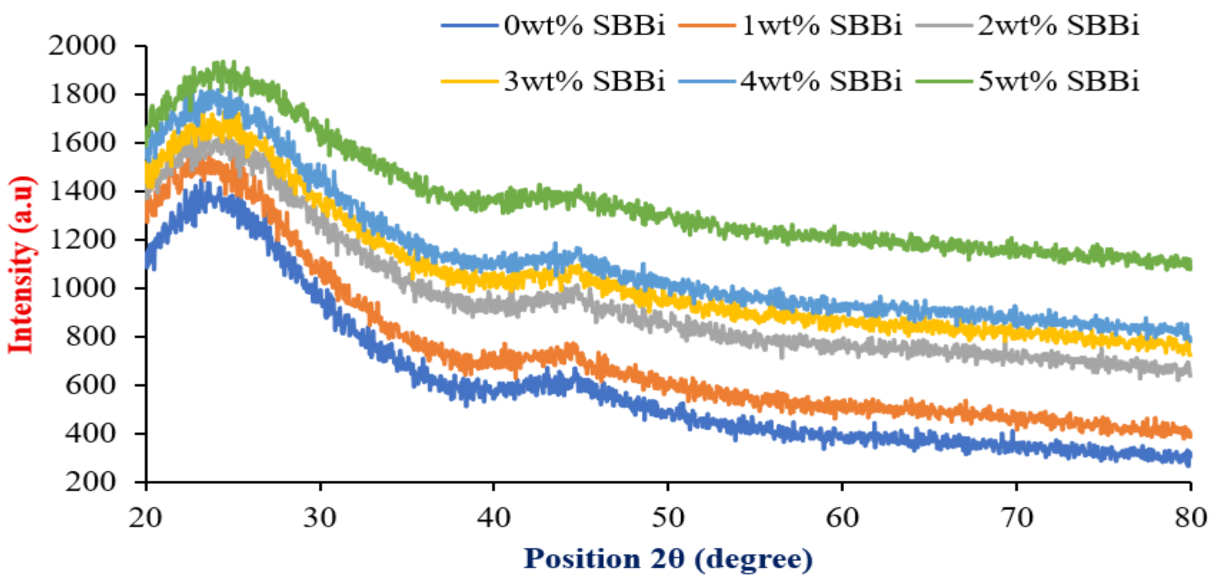

Figure 2: XRD patterns for Bi_2O_3 doped SLS borate glass system

XRD analysis

Figure 2 presents the XRD spectral pattern for the bismuth oxide doped SLS borate glasses recorded at room temperature, over 2θ position between 20 to 80 degrees. At lower scattering angles of $20^0 \leq 2\theta \leq 30^0$, the pattern showed a broad diffusion, indicating the existence of a long-ranged disorder. This indicates the absence of crystalline phase, confirming the amorphous nature of the glasses [26, 27]. It can be seen that the broad hump continued to become more broader with increase in the Bi_2O_3. This increase in the broadening of the hump indicates that the glasses becomes more amorphous than crystalline as the bismuth oxide composition is increased [27, 28].

Radiation shielding parameters

Table 2 and Fig. 3 respectively present the values and variation of linear attenuation coefficient as a function of Bi_2O_3 % composition. The LAC value increased from 0.0624 to 0.1277 cm^{-1} as the Bi_2O_3 % composition increased from 0 to 4 % and the dropped down to 0.1258 cm^{-1} when the composition rose to 5 %. The LAC was determined by measuring the intensity of gamma rays from a Cs-137 source after passing through given thickness of the glass sample.

Table 2: Initial radiation intensity, (I_o), final radiation intensity (I), sample thickness (x), linear attenuation coefficient (LAC) and mass attenuation coefficient (MAC) of Bi2O3 doped SLS borate glasses

Bi_2O_3 %	Intensity (I_o)	Intensity (I)	x (cm)	LAC (cm^{-1})	MAC (cm^2g^{-1})
0	14.46	13.9	0.633	0.0624	0.0276
1	14.46	13.86	0.512	0.0828	0.0355
2	14.46	13.7	0.557	0.0969	0.0414
3	14.46	13.46	0.628	0.1141	0.0485
4	14.46	13.4	0.596	0.1277	0.0532
5	14.46	13.34	0.641	0.1258	0.0522

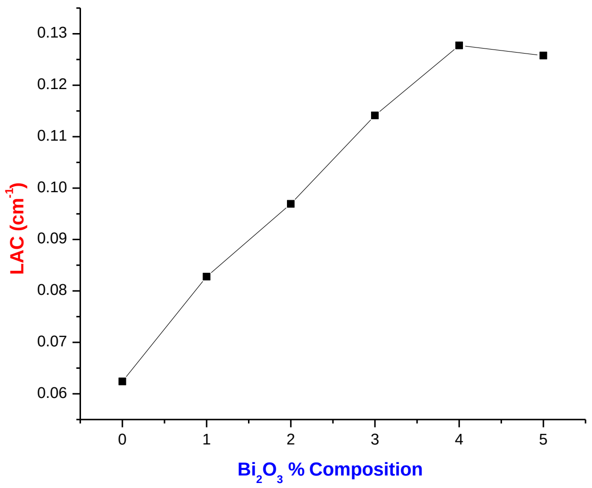

Figure 3: LAC variation against Bi_2O_3 % composition of Bi_2O_3 doped SLS borate glasses

The LAC was determined using equation (2) as presented by Aliyu *et al.* [24]. It predicts the possibility or probability of photon interaction per unit length of a material, and it is expressed in cm^{-1} [29].

$$\text{LAC } (\mu) = \frac{1}{x}\ln\left(\frac{I}{I_0}\right) \quad (2)$$

Where: μ is the LAC, I and I_0 are the gamma radiation intensity after passing through the sample and before passing through the sample and x is the sample thickness

The initial rise in the value of LAC with increasing population of Bi atoms in the network which falls in line with submission of Geidam *et al.* [1] that suggested that more heavy atoms concentration increases LAC value for glasses.

The MAC values and variation with Bi_2O_3 % composition in Bi_2O_3 doped SLS borate glasses. The value rose from 0.0276 to 0.0532 cm^2g^{-1} and decreased down to 0.0522 as the Bi_2O_3 % composition increased from 0 to 4 % and up to 5 %, respectively.

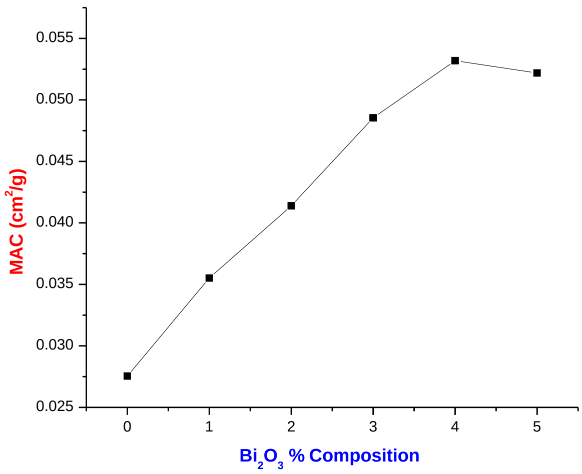

Figure 4: MAC variation against Bi_2O_3 % composition of Bi_2O_3 doped SLS borate glasses

The MAC (μ_m) was determined using equation (3) as presented by Thakur *et al.* [21]

$$\mu_m = \mu\rho^{-1} \quad (3)$$

The MAC of a material describes it's photon penetration and interaction inside the material [30].

The increase in the μ_m value with the increase in Bi_2O_3 % composition suggests that with more Bi ions added to the composition, the glasses' attenuation power becomes higher [31].

Table 3: Half value layer (HVL), tenth value layer (TVL), mean free path (MFP), permeability factor (PF) and radiation protection efficiency (RPE) of Bi_2O_3 doped SLS borate glasses

Bi_2O_3 %	HVL (cm)	TVL (cm)	MFP (cm)	PF (%)	RPE (%)
0	11.1086	36.9021	16.0264	96.1273	3.8728
1	8.37418	27.8184	12.0814	95.8506	4.1494
2	7.15096	23.7550	10.3167	94.7441	5.2559
3	6.07414	20.1779	8.76313	93.0844	6.9156
4	5.42634	18.0259	7.82856	92.6694	7.3306
5	5.51119	18.3078	7.95096	92.2545	7.7455

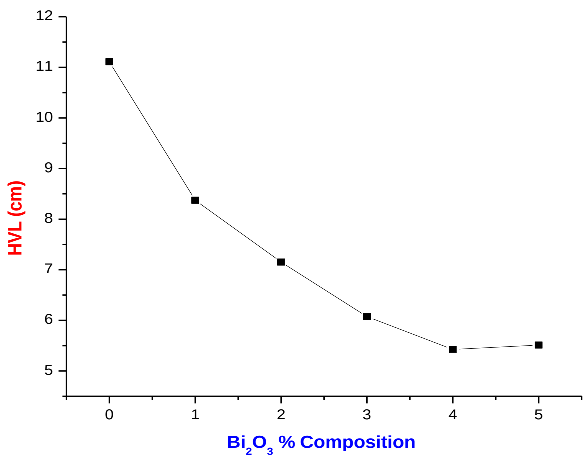

Figure 5: HVL variation against Bi_2O_3 % composition of Bi_2O_3 doped SLS borate glasses

The values and variation of the HVL against the Bi_2O_3 % Composition are presented in Table 3 and Fig. 5, respectively. The value showed a decreasing pattern from 11.1086 to 5.42634 cm and then increased to 5.51119 cm. The HVL was determined using equation (4) as presented by Deng *et al*. [32] as follows;

$$HVL = \frac{ln2}{\mu} \quad (4)$$

Decrease in HVL indicates an increase in the probability of the occurrence of Compton scattering and thus suggesting more shielding ability of the glasses. The reported increase in the value as the Bi_2O_3 % composition to 5 % might be due to increased interstitial spaces between atoms resulting in a decrease in density and thus the HVL [31, 33].

Figure 6 presents the graph of tenth value layer (TVL) versus Bi_2O_3 % composition and the values are contained in Table 3. This parameter represents the material's thickness that is needed to bring down the intensity of radiation to one-tenth of the original value before passing through the material [34].

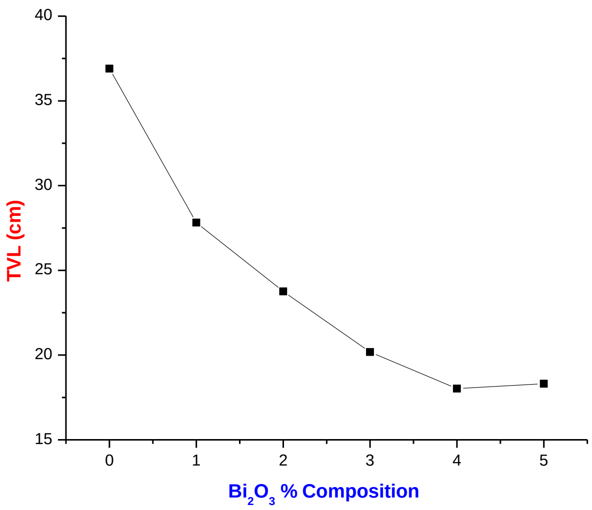

Figure 6: TVL variation against Bi_2O_3 % composition of Bi_2O_3 doped SLS borate glasses

The TVL values are determined using equation (5) as presented by Vadavathi *et al*. [30],

$$TVL = \frac{\ln 10}{\mu} \quad (5)$$

The TVL value decreased from 36.9021 to 18.0259 cm as the Bi_2O_3 % composition increased from 0 to 4 % and increased to 18.3078 cm when the Bi_2O_3 % composition rose to 5 %. The initial decrease in the TVL indicates an increase in the shielding performance of the glasses with Bi ions concentration increase, while the decrease indicates otherwise [35].

The values and variation of MFP with Bi_2O_3 % composition are presented in Table 3 and Fig. 7, respectively. The value decreased from 16.0264 to 7.82856 cm as Bi_2O_3 % composition increased from 0 to 4 % and in then increased to 7.95096 when the Bi_2O_3 % composition was raised to 5 %. The MFP is a very important parameter that defines the distance traveled by a photon between successive collisions within the glass network structure [36].

MFP values were determined using equation (6) as presented by Rammah *et al*. [37];

$$MFP = \frac{1}{\mu} \quad (6)$$

The decrease in the MFP value with the increase in Bi^{3+} ions concentration in the glass structure increases the chances of photon to particle collision and decreases the chances of photon penetration through the glasses [38].

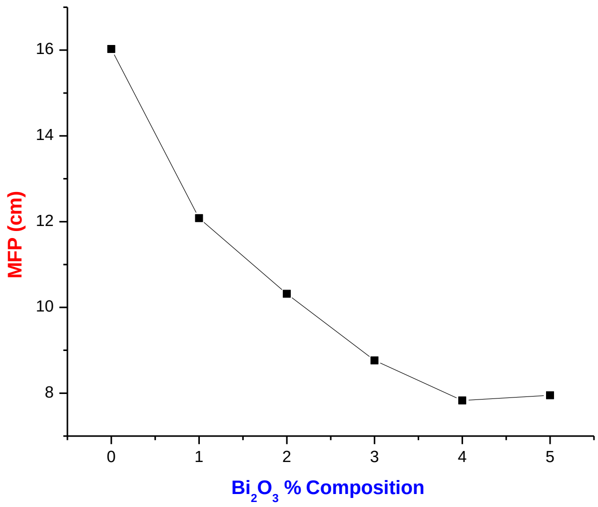

Figure 7: MFP variation against Bi_2O_3 % composition of Bi_2O_3 doped SLS borate glasses

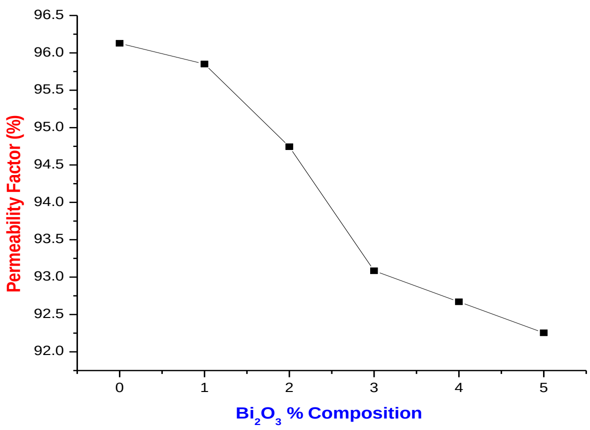

Figure 8: PF variation against Bi_2O_3 % composition of Bi_2O_3 doped SLS borate glasses

The permeability factor as a function of Bi_2O_3 % composition is presented in Fig. 8 and the values in Table 3. It is a parameter that represents the gamma radiation transmission ability of the glass at Cs-137 energy of 662 KeV [39].

The permeability factor (PF) is determined using equation (7) as presented by Al-jubbori *et al*. [39];

$$PF\ (\%) = \frac{I}{I_0}\ X\ 100 \quad (7)$$

The PF value decreased from 96.1273 to 92.2545 % as the Bi_2O_3 % composition increased from 0 to 5 %. This increase in the PF values translates to increase in the shielding efficiency due to the addition of more heavier Bi^{3+} ions that cover up more interstitial spaces within the glass network [34, 39].

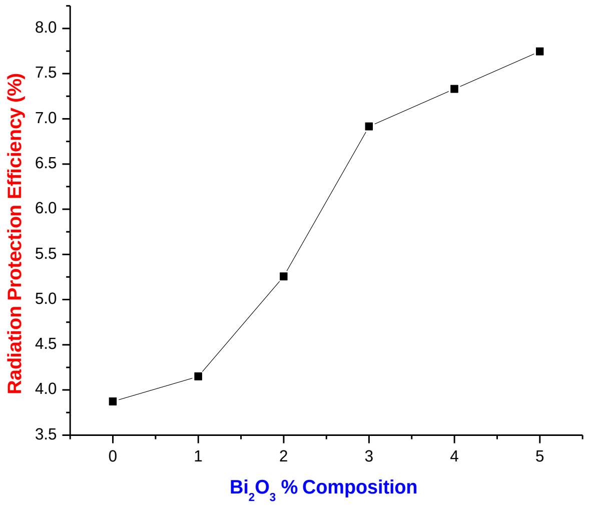

Figure 9: RPE Variation against Bi_2O_3 % Composition of Bi_2O_3 doped SLS Borate Glasses

Radiation protection efficiency values are presented in Table 3 and the variation against Bi_2O_3 % composition in Fig. 9. It represents the percentage of radiation intensity shielded over the total incident radiation intensity.
The RPE values were determined using equation (8) as follows [39];

$$RPE\ (\%) = \left(1 - \frac{I}{I_0}\right) X\ 100 \qquad (8)$$

The RPE value increased from 3.8728 to 7.7455 % with increase in the Bi_2O_3 % composition from 0 to 5 %.

Comparative density LAC, MAC and HVL data from different glasses

Table 4: Camparison between density, MAC, LAC and HVL for various compositions of glasses containing Bi_2O_3

Composition	Density (gcm^{-3})	MAC (cm^2g^{-1})	LAC (cm^{-1})	HVL (cm)	Reference
xBi_2O_3-(1-x)B_2O_3, Bi_2O_3 = 25 %, E = 662 keV	5.543	0.0985	-	1.27	[7]
(55 – x) B_2O_3 -15 Bi_2O_3 -5 V_2O_5 -25 Na_2O -x (CBD) for Bi_2O_3 = 15 %, E = 59.5 keV	2.650	0.931	2.395	-	[13]
xY_2O_3-15Li_2O-15ZnO-5Bi_2O_3- (65-x)P_2O_5	2.9407	-	-	-	[40]
B_2O_3-Bi_2O_3-Na_2O-ZnO-La_2O_3 for Bi_2O_3 = 5 % & La_2O_3 = 1 %, E = 3000 keV	3.235	-	0.120	-	[35]
xBi_2O_3-(100-x)[50SLS-50B_2O_3] for Bi_2O_3 = 5 %, E = 662 keV	2.4099	0.0522	0.1258	5.5112	Present

Table 4 presents a table comparing the values the density, MAC, LAC and HVL of variety of glass composition to the present glasses. It can be shown that glasses with higher concentration of Bi_2O_3 results in higher glass density which consequently produced higher shielding efficiency in terms of LAC, MAC and HVL.

Conclusion

Radiation shielding properties of bismuth oxide doped SLS borate glasses synthesized using melt-quenching technique was studied in this paper. The objective was to ascertain the shielding efficiency of the SLS waste-based glasses. The physical and structural properties of the glasses were studied using density measurement and XRD analysis. The XRD spectra revealed no sharp peaks and suggested the glasses were all amorphous in nature. The LAC and MAC values ranged between 0.0624 to 0.1277 cm^{-1}, and 0.0276 to 0.0532 cm^2g^{-1}. Other gamma radiation shielding efficiency parameters studied include Half Value Layers (HVL), Mean Free Path (MFP), Tenth Value Layer (TVL), Permeability Factor (PF) and Radiation Protection Efficiency (RPE).

Conflict of interest: The authors have declared that there is no conflict of interest reported in this study.

Acknowledgment: This research was funded by the Tertiary Education Trust Fund (TETFund) of the Federal Republic of Nigeria under the TETFund Research Project Grant (Grant Number: FUL/REG?TETF/002/VOL.VI/360) for the project titled "Bismuth Doped Soda Lime Silica Borate (SLS-B_2O_3-Bi_2O_3) Glasses for Gamma Radiation Shielding Application."

References

[1] Geidam, I. G., Matori, K. A., Halimah, M. K., Chan, K. T., Muhammad, F. D., Ishak, M. & Umar, S. A. (2022). Oxide ion polarizabilities and gamma radiation shielding features of TeO_2–B_2O_3 – SiO_2 glasses containing Bi_2O_3 using Phy-X/PSD software. *Mater. Today Commun.*, 31, 1–9.

[2] El-Mallawany, R., Sayyed, M. I. & Dong, M. G. (2017). Comparative shielding properties of some tellurite glasses: Part 2. *J. Non. Cryst. Solids*, 474, 16–23, DOI: 10.1016/j.jnoncrysol.2017.08.011

[3] Sayyed, M. I., Tekin, H. O., Kılıcoglu, O., Agar, O. & Zaid, M. H. M. (2018). Shielding features of concrete types containing sepiolite mineral: Comprehensive study on experimental, XCOM and MCNPX results. *Results Phys.*, 11, 40–45. DOI: 10.1016/j.rinp.2018.08.029

[4] Azeez, A. B., Mohammed, K. S., Al Bakri, A. M. M., Hasan, H. I. & O. A. Abdulkareem, (2014). Radiation shielding characteristics of concretes incorporates different particle sizes of various waste materials. *Adv. Mater. Res.*, 925, 190–194. DOI: 10.4028/www.scientific.net/AMR.925.190

[5] Mahmoud, M., Makhlouf, S. A., Alshahrani, B., Yakout, H. A., Shaaban, K. S. & Wahab, E. A. A. (2021). Experimental and simulation investigations of mechanical properties and gamma radiation shielding of lithium cadmium gadolinium silicate glasses doped erbium ions. *Silicon*, 1–15.

[6] Saddeek, Y. B., Issa, S. A. M., Alharbi, T., Aly, K., Ahmad, M. & Tekin, H. O. (2020). Mechanical and nuclear shielding properties of sodium cadmium borate glasses: Impact of cadmium oxide additive. *Ceram. Int.*, 46(3), 2661–2669. DOI: 10.1016/j.ceramint.2019.09.254

[7] Vadavathi, A. M., Chinthakayala, S. K., Kollipara, V. S., Ramadurai, G. & Gadige, P. (2021). Physical properties and gamma radiation shielding capability of highly dense binary bismuth borate glasses. *Ceram. Int.*, vol. 47(7PA), 9791–9805. DOI: 10.1016/j.ceramint.2020.12.120

[8] Eyüp Zorla, Cagatay Ipbüker, Alex Biland, Madis Kiisk, Sergei Kovaljov, Alan H. Tkaczyk & Volodymyr Gulik, (2017). Radiation shielding properties of high performance concrete reinforced with basalt fibers infused with natural and enriched boron. *Nucl. Eng. Des.*, 313, 306–318. DOI: 10.1016/j.nucengdes.2016.12.029

[9] Alajeramia, Y. S., Drabold, D., Mhareb, M. H. A., Katherine Leslee A. Cimatu, Gang Chena & Kurudirek, M. (2020). Radiation shielding properties of bismuth borate glasses doped with different concentrations of cadmium oxides. *Ceram. Int.*, 46(8), 12718–12726. DOI: 10.1016/j.ceramint.2020.02.039

[10] Azuraida, A., Halimah, M. K., Ishakc, M., Hasnimulyati, L. & Ahmada, S. I. (2020). Gamma ray shielding parameter of barium-boro-tellurite glass. *Chalcogenide Lett.*, 17(4), 187–196.

[11] Kawa M. Kaky, M. Kh. Hamad, Taha Yaseen Wais, M.I. Sayyed, Israa Abed Jawad, Berivan F. Namaq, Muntadher Alsabah & Yasser Maghrbi (2026). Combined experimental and Geant4 Monte Carlo study of radiation shielding investigation of TeO_2-B_2O_3-ZnO-BaO-Bi_2O_3-PbO transparent glass-ceramic composition. *Chem. Phys. Impact*, 12, 101065. DOI: 10.1016/j.chphi.2026.101065

[12] Elsaman, R., Somaily, H. H. & Algarni, H. (2020). Mechanical, physical and gamma ray shielding properties of xPbO-(50-x) MoO3–50V2O5 ($25 \leq x \leq 45$ mol %) glass system. *Ceram. Int.*, 46(12), 20251–20263. DOI: 10.1016/j.ceramint.2020.05.107.

[13] Abdelgawad, K. R. M., Saleh, H. A., Elwan, R. L., Fayad, A. M. & Ahmed, R. M. (2026). Optical properties and multi-radiation shielding performance of cement dust incorporated bismuth-vanadium-borate glasses. *Nucl. Eng. Technol.*, 58(10), 104416. DOI: 10.1016/j.net.2026.104416

[14] Shreeshmal Bhavya, Sachin Shet, K. R. Vighnesh, R. Kiran, Ashwitha Nancy D'Souza, L. Ramu, Srinivas Shenoy Heckadka & Sudha D. Kamath (2026). Effect of glass composition on physical, mechanical and radiation shielding performance of Barium Bismuth Boro-tellurite glasses. *Results Phys.*, 81.

[15] Alomairy, S., Mutuwong, C., Boukhris, I., Olarinoye, I. O. & B. T. Tonguc, (2021). Effect of Nd_3 + ions on radiation attenuation properties of PbF_2–TeO_2–WO_3 glass system for shielding applications. *Boletín La Soc. Española cerámica y Vidr.*, 1–17, DOI: 10.1016/j.bsecv.2021.03.005

[16] Al-Buriahi, M. S., Sayyed, M. I. & Al-Hadeethi, Y. (2020). Role of TeO2 in radiation shielding characteristics of calcium boro-tellurite glasses," *Ceram. Int.*, vol. 46(9), 13622–13629. DOI: 10.1016/j.ceramint.2020.02.148

[17] Azuraida, A., Halimah, M. K., Ishak, M., Hasnimulyati, L. & Ahmad, S. I. (2020). Gamma ray shielding parameter of barium-boro-tellurite glass. *Chalcogenide Lett.*, 17(4), 187–196.

[18] Umar, S. A., Halimah, M. K., Chan, K. T., Amirah, A. A., Azlan, M. N., Grema, L. U. Hamza, A. M. & Ibrahim, G. G. (2019). Optical and structural properties of rice husk silicate incorporated borotellurite glasses doped with erbium oxide nanoparticles. *J. Mater. Sci. Mater. Electron.*, 30, 18606–18616. DOI:10.1007/s10854-019-02213-z

[19] Salah Hassan Alazoumia, Sidek Abdul Aziza, R. El-Mallawany, Umar Sa'ad Aliyu, Halimah Mohamed Kamari, Mohd Hafiz Mohd Mohd Zaida, Khamirul Amin Matoria & Abdulbaset Ushah (2018). Optical properties of zinc lead tellurite glasses. *Results Phys.*, 9, 1371–1376. DOI: 10.1016/j.rinp.2018.04.041

[20] Umar, S. A., Halimah, M. K., Hamza, A. M. & Abdulbaset, A. A. (2018). The Structural, physical and optical properties of borotellurite glasses incorporated with silica from rice husk. *J. Sci. Math. Lett.*, 6, 32–46.

[21] Thakur, S., Thakur, V., Singh, L., Ahmad, A. F., Aliyu, U. S., Tafida, R. A. & Prasad, A. S. S. (2023). Thermo- and photoluminescent properties and gamma radiation shielding efficiency of NiO doped B_2O_3–Bi_2O_3 glass system. *Radiat. Phys. Chem.*, 216. https://doi.org/10.1016/j.radphyschem.2023.111402

[22] Halimah, M. K., Awshah, A. A., Hamza, A. M., Umar, S. A., Chan, K. T. & Alazoumi, S. H. (2020). Effect of neodymium nanoparticles on optical properties of zinc tellurite glass system. *J. Mater. Sci. Mater. Electron.*, 31, 3785–3794 DOI: 10.1007/s10854-020-02907-9

[23] Alazoumi, S. H., Umar, S. A., Ahmad, A. F., Sidek, H. A. A., Awshah, A. A., Thakur, S. & Geidam, I. G. (2024). Structural, elastic, thermo-physical and gamma radiation shielding efficiency of MnO_2 doped TeO_2-PbO-ZnO glasses. *Opt. Mater. (Amst).*, 150, 115277. DOI: 10.1016/j.optmat.2024.115277

[24] Aliyu, A. S., Hamza, A. M., Dunama, A. M., Aliyu, U. S., Nyakuma, B. B., Gaya, U. I., Musa, Y., Asuku, A., Saleh, I. M., Zira, J. D., L iman, M. M. & Liman, M. S. (2024). Optoelectronic and gamma ray attenuation properties of ore-based Bi and Sn-doped borosilicate glasses. *Ceram. Int.*, 50(15), 26424–26434. DOI: 10.1016/j.ceramint.2024.04.369

[25] Geidam, I. G., Matori, K. A., Halimah, M. K., Chan, K. T., Muhammad, F. D., Ishak, M., Umar, S. A. & Hamza, A. M. (2021). Thermo-physical and elastic properties of Bi2O3 doped silica borotellurite glasses. *Optik (Stuttg).*, 248, 168201. DOI: 10.1016/j.ijleo.2021.168201

[26] Shaaria, H. R., Azlana, M. N., Azlina, Y., N. M. Al-Hadab, S. A. Umarc, B. K. Kenzhaliyevd, Zaide, M. H. M., Hisamf, R. & Yusofg, N. N. (2022). Oxide ion polarizability, optical basicity, and metallization criterion of GO-coated Nd_2O_3 (NPs) - TeO_2 glass for linear optical fibre. *Chalcogen. Lett.*, 19(8), 565–577

[27] Azlan, M. N., Halimah, M. K., Suriani, A. B., Azlina, Y., Umar, S. A. & El-mallawany, R. (2019). Upconversion properties of erbium nanoparticles doped tellurite glasses for high efficient laser glass. *Opt. Commun.*, 448, 82–88. DOI: 10.1016/j.optcom.2019.05.022

[28] Aliyu, A. S., Dunama, A. M., Aliyu, U. S., Hamza, A. M., Nyakuma, B. B., Gaya, U. I., Zira, J. D., Liman, M. M., Liman, M. S. Lorbee, V. J. (2024). Bismuthite and cassiterite-doped borosilicate glass systems for X-rays attenuation : Fabrication and characterisation. *Opt. Mater. (Amst).*, 151, 115365. DOI: 10.1016/j.optmat.2024.115365

[29] Hanfi, M. Y., Issa, S. A. M., More, C. V & Sayyed, M. I. (2026). Experimental assessment of gamma-ray attenuation features of BaO-CaO-enriched borate glasses as lead-free radiation shielding materials. *Nucl. Eng. Technol.*, 58.

[30] Rao, L. S. (2025). Modifier effect of $BaTiO_3$ nanoparticles on morphology, structural, and radiation shielding characteristics of Li_2O–$BaTiO_3$–B_2O_3: TiO_2 glasses. *Nucl. Eng. Technol.*, 58. DOI: 10.1016/j.net.2025.103905

[31] Sayyed, M. I., Marashdeh, M. W., Kumar, A. & Yasmin, S. (2026). Tailoring the structural and functional properties of B_2O_3-PbO_2-BaO-CaO-Sm_2O_3 glass system for potential radiation shielding applications. *J. Sci. Adv. Mater. Devices*, vol. 11(1), 101082. DOI: 10.1016/j.jsamd.2025.101082

[32] Denga, H., Ganb, R., Miyazakic, H., Berglerd, M., Okab, R., de Lignya, D., Hayakawab, T. & Cicconia, M. R. (2025). Structure – property relationships in Bi_2 O_3 – TiO_2 – B_2O_3 glasses modified with BaO: toward lead – free radiation shielding materials. *Ceram. Int.*, 51(30PA), 63427–63440. DOI: 10.1016/j.ceramint.2025.11.129

[33] Mukamil, S., Ullah, I., Sarumaha, C., Wabaidur, S. M., Islam, M. A., Khatta, S. A., Kothan, S., Shoaib, M., Khan, I., Ullah, I., Kaewkhao, J. & Rooh, G. (2022). Lead-borate glass system doped with Sm^{3+} ions for the X-ray shielding applications. *Results Phys.*, 43, 106121. DOI: 10.1016/j.rinp.2022.106121

[34] Ali M. Onaizi, Mugahed Amran, Waiching Tang, Nour Betoush, Mohammad Alhassan, Raizal S. M. Rashid, Mohammad Fares Yasin, Bayagoob, K. H. & Sagheer A. Onaizi (2024). Radiation-shielding concrete: A review of materials, performance, and the impact of radiation on concrete properties. *J. Build. Eng.*, vol. 97, 110800. DOI: 10.1016/j.jobe.2024.110800

[35] Sayyed, M. I., Alshamari, A. & Mhareb, M. H. A. (2025). Roles of ZnO and La 2 O 3 in enhancing the mechanical, optical, and radiation shielding properties of B2O3 -Bi2O3 -Na2O transparent glasses. *J. Radiat. Res. Appl. Sci.*, 18(4), 101859. DOI: 10.1016/j.jrras.2025.101859

[36] Kebaili, I., Boukhris, I., Al-buriahi, M. S., Alalawi, A. & Sayyed, M. I. (2021). Ge-Se-Sb-Ag chalcogenide glasses for nuclear radiation shielding applications. *Ceram. Int.*, 47(1), 1303–1309, DOI: 10.1016/j.ceramint.2020.08.251

[37] Rammah, Y. S., Kavaz, E., El Agawany, F. I., Tekin, H. O. & Peris, U. (2020). Nuclear radiation shielding using barium borosilicate glass ceramics. *J. Phys. Chem. Solids*, 142, DOI: 10.1016/j.jpcs.2020.109437.

[38] Almuqrin, A. H. & Sayyed, M. I. (2021). Radiation shielding characterizations and investigation of TeO_2–WO_3–Bi_2O_3 and TeO_2–WO_3–PbO glasses. *Appl. Phys. A Mater. Sci. Process.*, 127(3), 1–11. DOI: 10.1007/s00339-021-04344-9

[39] Al-jubbori, M. A. & Taha, M. (2026). Efficiency of radiation shielding for types automotive glass in the market Iraq: Experimental and theoretical study. *Next Mater.*, 12, 102155, DOI: 10.1016/j.nxmate.2026.102155

[40] Gharam A. Alharshan, Mamdouh I. Elamy, Shimaa Ali Said, A.M.A. Mahmoud, R.A. Elsad, Nasra M. Ebrahem, Islam M. Nabil (2025). Impact of yttrium on the optical and neutron radiation shielding properties of bismuth-lithium-zinc-phosphate glasses. *J. Radiat. Res. Appl. Sci.*, 18(4), 101891. DOI: 10.1016/j.jrras.2025.101891

Citing this Article

Aliyu, U. S., Geidam, I. G., Hamza, A. M., Muhammad, S., Muhammad, M. A., Ibrahim, H. S., & Liberty, M. B. (2026). Bismuth doped soda lime silica borate (SLS–B_2O_3–Bi_2O_3) glasses for gamma radiation shielding application. *Lafia Journal of Scientific and Industrial Research, 4*(2), 131–138. https://doi.org/10.62050/ljsir2026.v4n2.911